# Corrosion Behaviour of Al, Cu, and Fe Alloys in Deep Sea Environment

G. Luciano, P. Letardi, P. Traverso, L. Belsanti

*The aim of this study is to investigate deep sea environment effects on the corrosion of Al, Fe, and Cu alloys, employed in the KM3NeT project, a deep sea infrastructure designed to host a neutrino telescope. Alloys commonly used in seawater, as well as less widely employed materials were studied. Samples were immersed at the NEMO site (located off Capo Passero, Italy; 3365 m depth) for consecutive time periods of 6, 12 and 18 months. A representative set of samples was recovered and laboratory tests performed to evaluate the type and degree of corrosion attack. Stainless steels reported the best performance in terms of weight loss, corrosion rate, and corrosion morphology. However, also Al 5093 and Al 6082 performed satisfactorily, in terms of weight loss and corrosion rate. This prescreening will be partially employed in selecting building materials for the KM3NeT structure.*

INTRODUCTION

The chemical and physical characteristics of deep-sea environment are significantly different from surface sea water. Pressure is the greatest physical force acting in deep-sea environment: it increases by 1 atm every 10 m depth. Generally, also salinity increases with depth. Conversely, deep-sea temperature, oxygen content, and pH are lower than in surface water [1,2].

Due to these peculiarities, more in situ deep sea corrosion studies are urgently required, despite all the difficulties to perform them, their high experimental costs, and long testing periods. This is also the reason why there are so few of them in the literature, compared with the large amount of research works on corrosion in shallow sea water.

The available literature can be classified into 3 different fields:

a)  Experiments performed in deep sea;
b)  Experiments performed in laboratory to simulate deep sea conditions;
c)  Characterisation of shipwreck and archaeological artefacts found on the sea bottom

We will mainly focus on a) and b) papers, since the materials and the methodology described are closer to this study. Reinhart pioneered this field with the most comprehensive

investigation to date [2]. In his report published in 1976, the results of tests performed in the Pacific Ocean between 1960 and 1970 on about 20,000 specimens of 475 different alloys were presented. The test specimens included steels, cast irons, stainless steels, copper, nickel, aluminium, titanium, miscellaneous alloys, and wire ropes. Summarizing the conclusions, the mechanism of corrosion was strictly related to different oxygen content in the water column. Pressure had instead a negligible effect on the corrosion behaviour of almost all alloys.

More recent works performed in the Arabian Sea and the Indian Ocean by Sawant et al. showed that the corrosion rates of mild steel and brass increase with depth, whereas corrosion rate decreases with increasing depth in the case of aluminium alloys and stainless steels [1,3,4]. Venkatesan et al. concluded that depth had no influence on the corrosion of ferrous alloys [1].

All the above cited studies agree that the most important feature affecting corrosion rate is the oxygen content profile, which varies with depth.

Simulated laboratory experiments performed by Beccaria et al. both in seawater and in 3.5 % NaCl solution achieved different results than those obtained by Reinhart, since they pointed to an influence of pressure on corrosion rate [5,6,7,8,9].

They stated that by increasing the pressure from 1 to 300 atm, the corrosion rate of copper, brass and zinc increased. They assumed that the increase of corrosion rate with pressure was due to the acceleration of the cathodic reduction process for copper, and to anodic process acceleration for brass alloy and for zinc. Nickel corrosion inhibition was also reported, with the formation of a passivating layer with a

**Giorgio Luciano, Paola Letardi, Pierluigi Traverso**
*C.N.R.- I.S.MAR., via De Marini 6, I-16149 Genoa, Italy*

**Lucrezia Belsanti**
*C.N.R.- I.S.MAR., via De Marini 6, I-16149 Genoa, Italy*
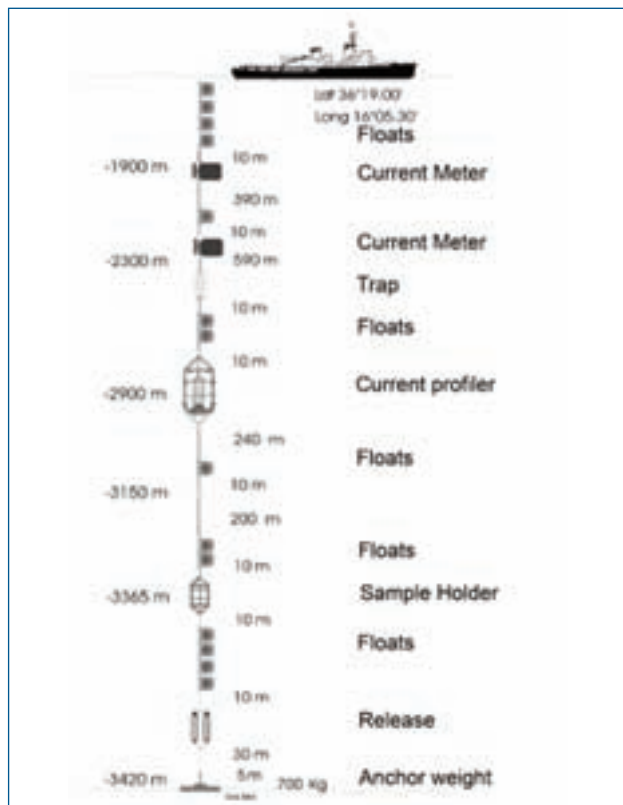*I.S.P.R.A., via Vitaliano Brancati 48, I-00144 Rome, Italy*

*Figure 1: Mooring line used in field tests.*



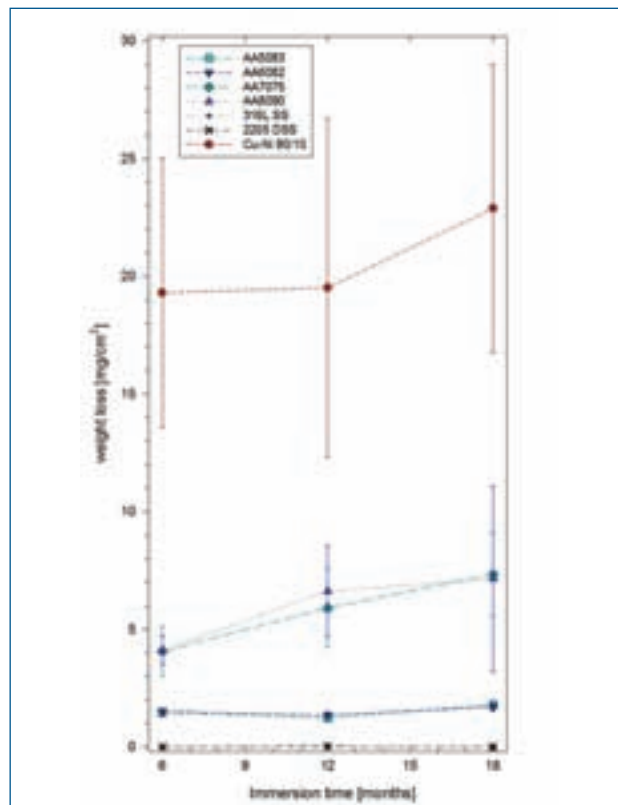*Figure 2 Normalized weight loss comparison for all investigated alloys, as a function of immersion time in deep sea water.*

greater dielectric constant than those formed at ambient pressure. A different susceptibility to pitting in some aluminium alloys was correlated to the composition and morphology of the oxidation layer.

Further, for nickel and some aluminium alloys, they also found that the mechanism of oxide formation on the metal surface changed depending on the hydrostatic pressure applied to the specimens.

In the light of the above discussed results, more investigations are necessary aimed at evaluating the amount and the type of degradation on selected materials in the site of interest.

Accordingly, the aim of this work is to investigate the effects of natural deep-sea environment on the corrosion of some commercial aluminium, copper, and iron alloys. Actually, this study is related to the design of KM3NeT, a European deep-sea research infrastructure that will host a neutrino telescope with a volume of at least one cubic kilometre, at the bottom of the Mediterranean Sea. The facility will also house instruments and equipment for earth and marine sciences for long term and on-line monitoring of the deep sea environment and the sea bottom at a depth of

| pH | ~7.9 |
| potential temperature | ~ 13.4 °C |
| salinity | 38.7 g/L |
| dissolved oxygen | 4.7 mL/L |

several kilometres [10]. A detailed description of the corrosion mechanism is beyond the aim of this paper since, in order to do so, more site-specific parameters should have been monitored. However, for lack of time, it was not possible to collect more data on the immersion site.

## MATERIALS AND METHODS

Materials included alloys commonly used in seawater, although some materials that are not generally employed for this specific application were also selected. Several sets of specimens were exposed for three different periods: 6, 12, and 18 months. Each set was composed of 4 samples of the same material for each exposure time, 3 samples for weight loss assessment, and 1 for morphological analyses. Nominal composition (weight %) and heat treatment of the alloys selected for the study are reported in Table 1. The approximate size of each sample was 100x100mm, with 2 to 5 mm thickness, depending on the alloy.

A general view and the feasibility study of these experimental tests were presented in a previous work [11].

As soon as the samples were received from suppliers (the nominal composition of the alloy is shown in Tab. 1), they were rinsed in methanol in ultrasonic bath, dried, weighed with an analytical scale, and then fixed on 3 specially designed cylindrical anodized aluminum cages (about 1 meter high, 0.5 meter diameter). The specimens were hung with plastic fasteners on drilling holes of 6 mm diameter at the four corners of the samples. Special care was taken to ensure that they did not touch any other metal. Each cage was

| Al alloy | Al | Cu | Fe | Mn | Mg | Si | Zn | Cr | Ti | Li | Zr |
|---|---|---|---|---|---|---|---|---|---|---|---|
| AA 5083 H111 (1) | balance | 0.01 | 0.04 | 0.40-1.0 | 4.0-4.9 | 0.04 | 0.25 | 0.05-0.25 | 0.15 | - | - |
| AA 6082 T6 (2) | balance | 0.01 | 0.05 | 0.40-1.0 | 0.6-1.2 | 0.7-1.3 | 0.02 | 0.25 | 0.01 | - | - |
| AA 7075 T651 (3) | balance | 1.2-2.0 | 0.05 | 0.03 | 2.1-2.9 | 0.04 | 5.1-6.1 | 0.18-0.28 | 0.02 | - | - |
| AA 8090 T81 (4) | balance | 1.0-1.6 | ≤0.30 | ≤0.10 | 0.6-1.3 | ≤0.20 | ≤0.25 | ≤0.10 | ≤0.10 | 2.2-2.7 | 0.04-0.16 |
|  |  |  |  |  |  |  |  |  |  |  |  |
| Fe alloy | Fe | C | Mn | P | S | Si | Ni | Cr | Mo | N |  |
| 316 L SS | balance | ≤0.03 | ≤2 | ≤0.045 | ≤0.03 | ≤1 | 10.0-13.0 | 16.5-18.5 | 2.0-2.5 | - |  |
| 2205 DSS | balance | 0.03 | 1.46 | 0.025 | 0.002 | 0.56 | 5.04 | 0.969 | 3.19 | 0.16 |  |
|  |  |  |  |  |  |  |  |  |  |  |  |
| Cu Alloy | Cu | C | Mn | P | S | Fe | Ni | Zn | Pb |  |  |
| Cu-Ni 90/10 | balance | 0.001 | 0.062 | 0.007 | 0.004 | 0.086 | 10.36 | 0.014 | 0.004 |  |  |

*Table 1: Chemical composition (weight%) of the alloys chosen for the study. (1) H111 Annealed and slightly strain-hardened (less than H11) during subsequent operations such as stretching or levelling. (2) T6 Solution heat-treated and then artificially aged. (3) T651 Solution heat-treated, stress-relieved by controlled stretching (permanent set 0.5% to 3% for sheet) and then artificially aged. The products receive no further straightening after stretching. (4) T81 Solution heat treated, cold worked and then artificially aged.*

| Alloy |  | AA 5083 H111 | AA 6082 T6 | AA 7075 T651 | AA 8090 T81 | 316 L SS | 2205 DSS | Cu-Ni 90/10 |
|---|---|---|---|---|---|---|---|---|
|  | 6m | 1.5±0.1 | 1.5±0.1 | 4±1 | 4.1±0.6 | -0.003±0.002 | 0.007±0.002 | 19±6 |
|  | 12m | 1.2±0.1 | 1.3±0.2 | 6±2 | 7±2 | 0.002±0.002 | 0.026±0.004 | 20±7 |
|  | 18m | 1.8±0.1 | 1.7±0.2 | 7±2 | 7±4 | 0.01±0.01 | -0.007±0.003 | 23±7 |

*Table 2: Weight Loss (mg/cm² ) of different materials as a function of immersion time in deep sea water.*

filled with the same sample selection of materials to be investigated.

Specimens were exposed by means of a deep sea mooring line at 3,365 m depth (at 55 m from sea bottom) at the NEMO site [10], located off Capo Passero (Sicily, Italy) in the West Ionian Sea at 36° 16' N 16° 06' E. The typical layout for the used mooring line is shown in Figure 1.

The most important average parameters that were measured "in situ" during immersion time are reported below:

For a detailed site description including physical and chemical analysis, see [12,13,14,15]. It is useful to point out that potential temperature can be defined as the temperature which a water parcel has when moved adiabatically to another pressure. In the ocean, we commonly use the sea surface as our 'reference' pressure for potential temperature: temperature values of parcels are compared as if they had been moved, without mixing or diffusion, to the sea surface.

At each exposure time, one of the cages housing the samples was retrieved from the mooring line.

After recovery, each cage was cleaned with fresh water and then dried on the ship deck. The specimens were successively brought to the laboratory, mechanically polished with a soft bristle brush under running water, in order to remove lightly adhering deposits and bulky corrosion products, and then washed with distilled water and dried before weighing, according to ISO 8407:1991(E). All corrosion products were removed with the above treatment; no further treatment was necessary.

In order to evaluate the type and extent of corrosive attack, the following laboratory investigations were performed:
a) weight loss and corrosion rate calculation;
b) digital photographs;
c) OM examination;
d) SEM-EDX analyses on selected samples.

Samples were weighed with an analytical scale (Mettler H 315, up to 0.1 mg accuracy), and the weight loss of every sample was normalized to the surface area.

The following formula was used for corrosion rate (CR) calculation [15]:

$$CR = \frac{K \cdot W}{A \cdot T \cdot D}$$

| Immersion time (months) | AA 5083 H111 | AA 6082 T6 | AA 7075 T651 | AA 8090 T81 | 316 L SS | 2205 DSS | Cu-Ni 90/10 |
|---|---|---|---|---|---|---|---|
| 6 | 11±2 | 11±2 | 28±9 | 32±7 | 0±0 | 0±0 | 42±14 |
| 12 | 5±1 | 5±1 | 21±7 | 26±9 | 0±0 | 0±0 | 21±9 |
| 18 | 4±1 | 4±1 | 17±5 | 18±11 | 0±0 | 0±0 | 17±5 |

*Table 3: Corrosion rate ( m/year) of different materials as a function of immersion time in deep sea water.*

| Spectrum | O | Mg | Al | Fe | Cu | Zn | Total |
|---|---|---|---|---|---|---|---|
| 1 | 13.40 | 0.37 | 21.48 | 9.27 | 55.48 | | 100.00 |
| 2 | 0.84 | 2.21 | 88.74 | | 1.25 | 6.96 | 100.00 |

*Table 4: Weight % of elements revealed by EDS analyses of point 1 (inclusion) and point 2 (matrix).*

| Spectrum | Mg | Al | Ti | Cu | Zr | Total |
|---|---|---|---|---|---|---|
| 1 | | 63.18 | 5.11 | 0.79 | 30.93 | 100.00 |
| 2 | 0.55 | 98.19 | | 1.27 | | 100.00 |

*Table 5: Weight % of elements revealed by EDS analyses of  point 1 (inclusion) and point 2 (matrix).*

where CR is expressed in mm per year, K is a constant and it is the number of hours in one year, W is the mass loss in grams, A is the specimen area in $cm^2$, T is the exposure time expressed in hours, and D is the density in g $cm^{-3}$.

Pictures were taken of each sample before exposure and after different exposure periods. All the photographs were taken using a Canon EOS 500D with a Canon lens 50 mm f 1.7 and recorded at 12.2 MP in RAW format. To ensure high fidelity of reproduced colors, we calibrated the photos using ColorChecker(tm) workflow using a calibration card and the dedicated ColorChecker software inside Adobe(tm) Lightroom.

As to OM analyses, micrographies were taken using a Leica DM-RME system.

Representative specimens of AA 7075 and AA 8090 alloys, before and after 18 months of exposure, were prepared by cutting slices from the samples, in order to observe their morphology in backscattered electron mode, using a SEM (Leo 1450 VP) at 12 and 20 kV acceleration voltages. Micro-analyses using an EDX microprobe (Oxford INCA 300) were also carried out on these specimens, to better highlight localized corrosion morphology.

## RESULTS AND DISCUSSION

As already mentioned, in situ deep-sea corrosion studies are difficult to perform. Moreover, the deep ocean environment is a complex system: test outcome depends on a cumulative effect of environmental conditions, namely hydrostatic pressure, temperature, pH, dissolved oxygen, salinity, sea water current, suspended silt, decaying organic material, etc.. The individual effect on material corrosion of each of the above factors is not readily distinguishable. An overview of normalized weight loss and corrosion rate of all investigated alloys is reported in Figure 2 and Table 2 and 3, respectively, for comparison purposes.

These results show the wide corrosion resistance range of the different series of materials examined.
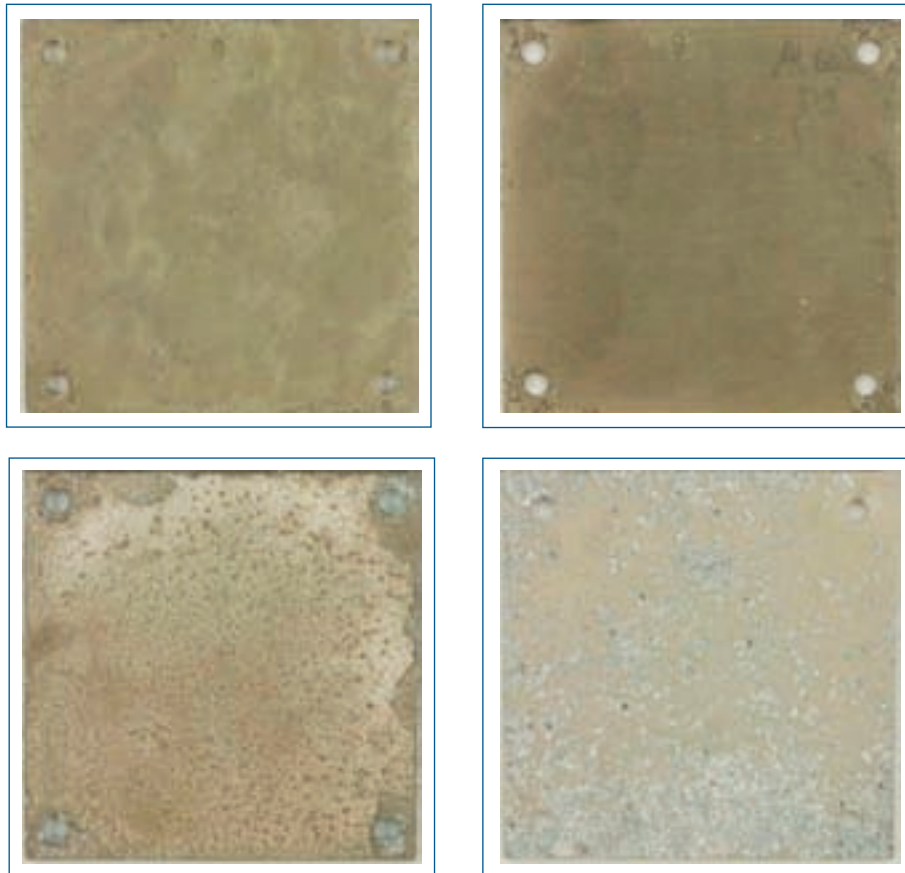
## AL ALLOYS

Among Al alloys, as expected, AA 5083 and AA 6082 alloys have shown the lowest weight loss and corrosion rate. For samples after 18 months of immersion time, AA 5083 alloy weight loss and corrosion rate average values are 1.8 $mg/cm^2$ and 4 µm/y, respectively, while they are 1.7 $mg/cm^2$ and 4 µm/y for AA 6082 alloy.

AA 7075 and Al-Li 8090 alloys performed poorly in comparison with the above mentioned alloys, with values of 7 $mg/cm^2$ and 17 µm/y, and 7 $mg/cm^2$ and 18 µm/y, respectively (Figure 2).

The results obtained are consistent with results found in the literature for shallow water corrosion rates [16].

Digital imaging of AA 5083 and AA 6082 alloys shows a slight change in texture, due to starting sites of pitting corrosion, only after 18 months of immersion (Figure 3 a) and b)). The AA 5083 and AA 6082 alloys show a quite similar morphology and a comparable degree of corrosion. OM examination clearly shows the presence of cracks in the superficial Al oxide layer (Figure 4 and 5).

After the same immersion time, a more aggressive pitting corrosion is observed on AA 7075 and AA 8090 alloys, with the noticeable presence of crystalline corrosion products (Figure 4 c) and d)). OM investigation shows details of severe localized and intergranular corrosion, on both AA 7075 and AA 8090 alloys, with the presence of a non homogeneous protective surface layer (Figure 6). SEM-EDS analyses were performed on representative areas of all samples. The surface morphology of AA 5083 and AA 6082 alloys confirms OM investigations. Indeed, cracks can be observed in surface oxide films (Figure 7,8)

The presence of inclusions can be observed in the AA 7075 alloy sample. EDS analyses were performed on both matrix (Figure 9, point 2; Table 4) and inclusions (Figure 10 point 1; Table 4).

Matrix composition is comparable with the alloy nominal composition, while inclusions mainly consist of Al and Cu. A similar behavior is found for AA 8090 alloy sample, in which inclusions are present. In this case too, EDS analyses were performed on both matrix (Figure 11, point 2; Table 5) and inclusions (Figure 11, point 1; Table 5). Matrix composition is comparable with the alloy nominal composition, while inclusions consist mainly of Al and Zr.

Inclusions act as corrosion starting sites.

Severe corrosion is due to microgalvanic coupling at the inclusions/alloy interfaces. However, the corrosion mechanism differs depending on the nature of the inclusion: Al-Cu intermetallic compounds act as a cathode stimulating galvanic corrosion. Conversely, Al-Zr inclusions act as anode. In this case, Al-Zr compounds dissolve and create physical defects, leading to the formation of low oxygen microcells that become sites of localized corrosion attack.
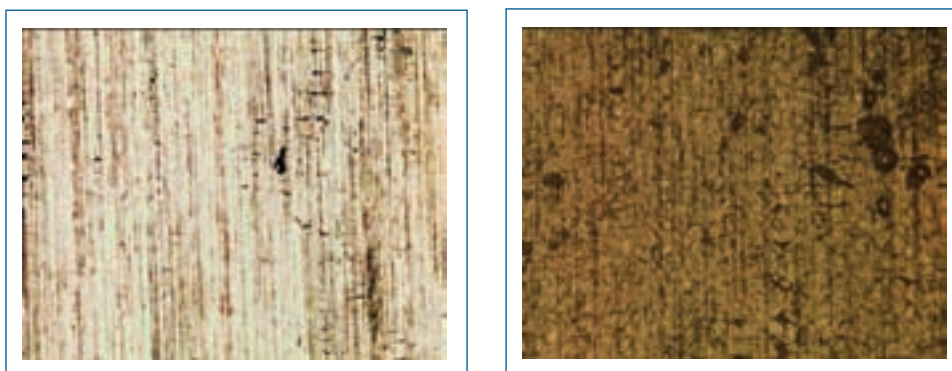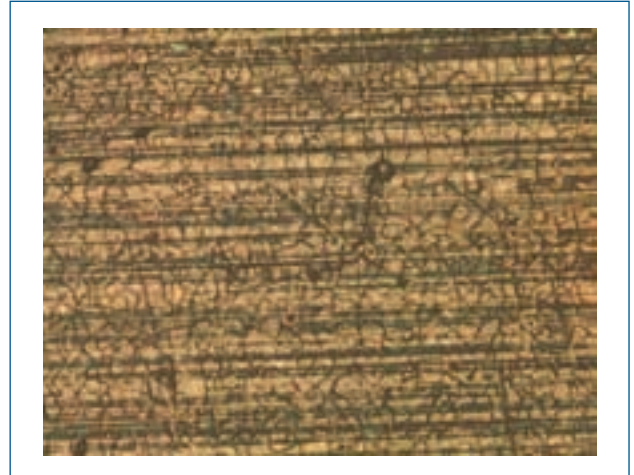
*Figure 5: OM (100x) of AA 6082 before (a) and after 18 months of deep sea immersion (b).*
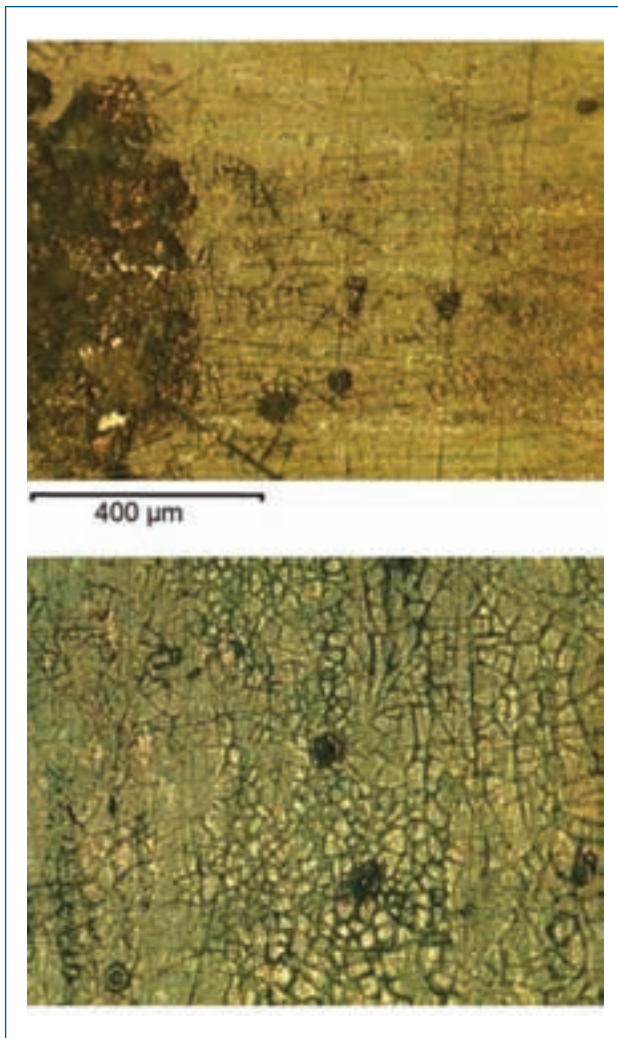


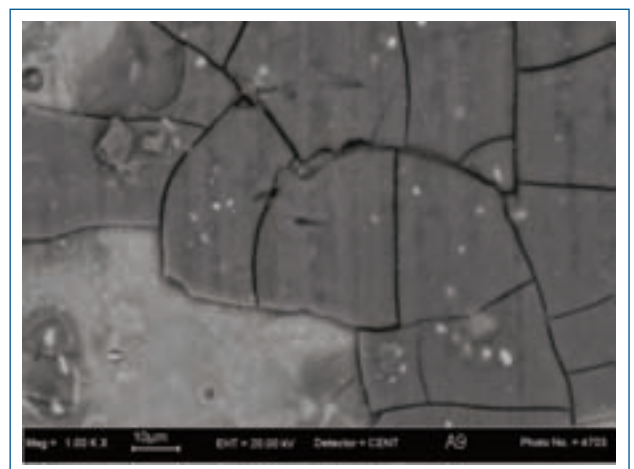*Figure 6: OM (100x) of AA 7075 after 18 months of deep sea immersion.*



*Figure 7: SEM of AA 5083 after 18 months of deep sea immersion. Cracks in the oxide surface layer are visible.*
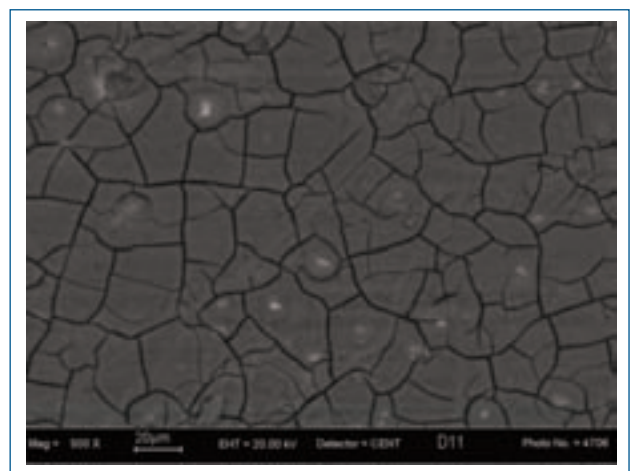


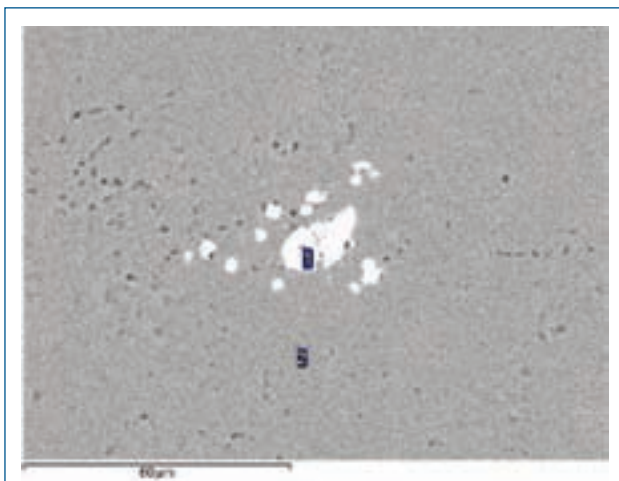*Figure 8: SEM of AA 6082 after 18 months of deep sea immersion. Crack in the oxide surface are visible.*

Some authors indicated that aluminum alloys in deep seawater have a similar corrosion behavior, although pit penetration rate could be higher and the effect of crevices somewhat greater [16]. Results on AA 5083 and AA 6082 alloys from our study well agree with reported data. As far as we know, no data have been reported in the literature on Al 8000 series in deep see water.

STAINLESS STEELS

With regard to the site physical-chemical parameters, we have found that there was enough oxygen content to maintain a passive film on our samples, which, after 18 months of immersion, had shown no change. Stainless steels are known to perform better in aerated seawater, since the lack of aeration at a specific site often leads to crevice attack. Very little oxygen is required to maintain the passive film on a clean stainless surface [15]. Stainless steels recorded almost no detectable weight loss (Figure 4), with negligible corrosion rate (Table 3). No significant degree of corrosion after 18 months of immersion is visible by digital imaging (Figure 12 a) and b)). Figure 13 a) and b) show the OM of the 316 L stainless steel before and after immersion (18
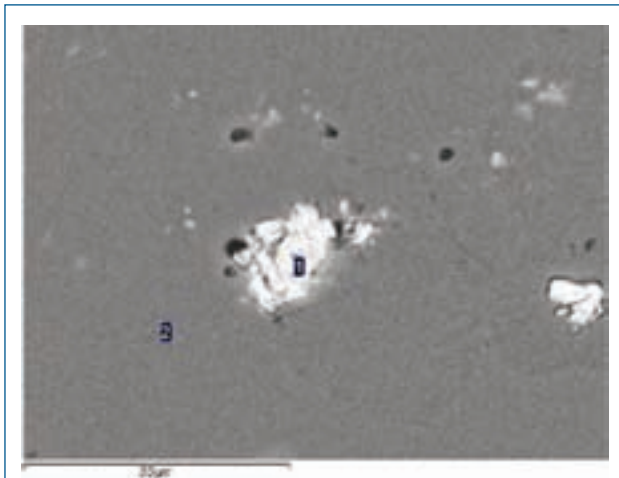


*Figure 9: SEM image of sample of AA 7075 in a non homogeneous area: point 1- inclusion, point 2- matrix.*



*Figure 10: SEM image of sample of AA 8090 in a non-homogeneous area: point 1- inclusion, point 2- matrix.*



*Figure 11: Stainless steel alloys after 18 months of deep sea immersion Sample size 100x100 mm a) 316 L SS; b) 2205 DSS.*

months); no significant differences are visible.
An isolated –not statistically significant - case of crevice corrosion was observed on one of the 12 month exposure samples, near the hooks used to fix the samples inside the cages (Figure 14).
Reinhart showed that the behavior of 300 series was very erratic and unpredictable, but that, in general, localized corrosion intensity was either about the same or greater at the surface than deeper down. The corrosion rate and weigh loss we have found are consistent with the results reported by him [2]
The results obtained for the duplex 2205 were the same as those obtained for the 316 L stainless steel. Therefore, the same mechanism of corrosion is thought to be in place.

CU-NI ALLOYS

Cu-Ni 90/10 alloy shows a higher weight loss than all the other investigated alloys (Figure 3).
The photos in Figure 15 point to a general corrosion attack process.
Optical microscopy highlights a severe generalized corrosion and a non-homogeneous patina (Figure 15 a) and b).

*Figure 12: OM (100x) of the 316 L Stainless Steel before and after immersion 18 months of immersion.*

In this case, the dissolved oxygen content in seawater is too low to maintain a homogeneous and protective layer (as confirmed by OM and SEM).

The results obtained are consistent with those reported by Reinhart et al. [2] in relatively quiescent seawater (typically less than 50 μm/y). Also, in [16] corrosion rates of copper and copper-nickel alloys in deep sea were reported not to change significantly for dissolved oxygen contents in seawater between 1 and 6 mL/L. Consequently, their corrosion behavior is not significantly affected by changes in exposure depth.

CONCLUSIONS

In general, the morphological analysis performed by means of SEM does not show any form of microfouling settlement on any of the surfaces of analyzed samples. This is due to the distance from the seabed and the depth of immersion. The effect of any microbiological corrosion has no significant impact on collected results.

All the examined samples behave consistently with the results found in the literature [2]. Oxygen content of sea water at the immersion site level is the most relevant parameter.

By looking at weight loss, corrosion rate, and corrosion phenomena morphology, stainless steels performed better than the other alloys, showing only a negligible corrosion at-tack. Generally speaking, oxygen plays a dual role in stainless steel corrosion: it keeps the alloy passive, but, at the same time, promotes pitting propagation, when corrosion starts. In our case, the passive layer was maintained almost intact with no pitting.

We have observed a very good performance of AA 5083 and AA 6082 alloys, in terms of weight loss and corrosion rate. With regard to corrosion morphology of these alloys, mostly localized corrosion was observed.

AA 7075 and Al-Li 8090 performed poorly compared to AA 5083 and AA 6082, showing a very high corrosion rate, in accordance with the literature [16], in the form of exfoliation and pitting corrosion. This behavior can also be due to the presence of intermetallic compounds that stimulate localized attack. This also confirms that these alloys are not suitable for deep sea applications, and that they could result into mechanical failure if no suitable protection is adopted.

The selected copper alloy showed the highest weight loss rate. It seems that the corrosion mechanism was triggered by the formation of a poorly adherent, non homogeneous patina. The oxygen content in the site was not enough to maintain a homogeneous and protective layer on the surface of the samples as described in [2] .

The study was used to pre-screen the material that could be



*Figure 13: Crevice corrosion on sample 316 L SS after 12 months of deep sea immersion. Hole diameter: 6 mm.*



*Figure 14: Cu-Ni 90/10 alloy after 18 months of deep sea immersion. Sample size 100x100 mm.*
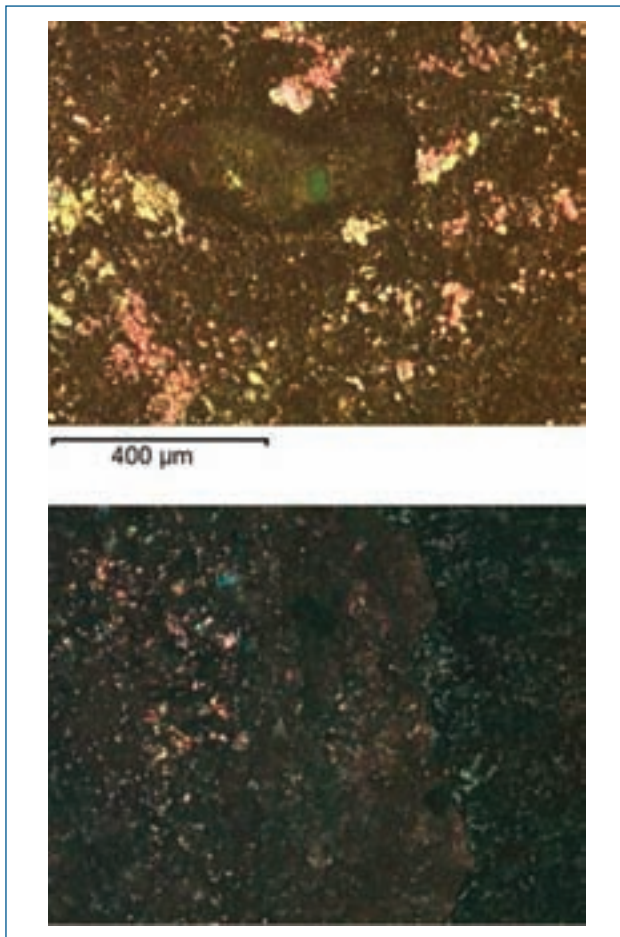
*Figure 15: OM (100x) of Cu-Ni 90/10 alloy after 18 months of deep sea immersion.*

employed to build the Km3net structure. For a more complete and reliable study, also engineering and economic data will be merged with the results presented here.

REFERENCES

[1]   R. VENKATESAN, M.A. VENKATASAMY, T.A. BHASKARAN, E.S. DWARAKADASA, M. RAVINDRAN, British Corros. J., 37 (2002), pp. 257-256.
[2]   F.M. REINHART,. Report Number TR-834, U.S. Department of Commerce, Civil Engineering Laboratory (Navy), 1976.
[3]   S.S. SAWANT, A.B. WAG, Corros. Prevent. Contr., 37 (1990), pp.154-157.
[4]   S.S. SAWANT, K. VENKAT, A.B. WAGH, Indian J. Technol., 1 (1993), pp. 862-866.
[5]   A.M. BECCARIA, G. POGGI, Corros. Prevent. Contr., (1987), pp. 51-57.
[6]   A.M. BECCARIA, P.L. TRAVERSO, G.POGGI, M.L. LORENZETTI, High. Pressure Res., 7 (1991), pp. 347-349.
[7]   A.M. BECCARIA, G. POGGI, M. ARFELLI, G. MATTOGNO, Corros. Sci., 34 (1993), pp. 989-1005.
[8]   A.M. BECCARIA, G. POGGI, D. GINGAUD, P. CASTELLO, British Corros. J., 29 (1994), pp. 65-69.
[9] A.M. BECCARIA, G. POGGI, P. CASTELLO, British Corros. J., 30 (1995), pp. 283-287.
[10] KM3NeT Consortium, Technical Design Report, preliminary version available on: http://www.km3net.org last access date 18/04/2012.
[11] M. FASSIN, P. TRAVERSO, La Metallurgia Italiana, (2008), pp. 29-38.
[12] S. SPARNOCCHIA, G. PIETRO GASPARINI, K. SCHROEDER, M. BORGHINI, Nuclear Instruments and Methods in Physics Research Section A: Accelerators, Spectrometers, Detectors and Associated Equipment, S87-S90 (2011), pp. 626-627.
[13] F. TOURATIER, C. GOYET, Deep Sea Research Part I: Oceanographic Research Papers, 58 (2011), pp. 1-15.
[14] P. RIVARO, R. MESSA, S. MASSOLO, R. FRACHE, Marine Chemistry, 121 (2010), pp. 236-245.
[15] M.M. (ed.) Schumacher, Seawater Corrosion Handbook, 1979.
[16] L.J. KORB, ASM, Metals Handbook, Ninth Edition: Volume 13 – Corrosion, 9th ed., ASM International, 1987.

**Resistenza alla corrosione di leghe Al, Cu, e Fe in ambiente marino ad alta profondità**

**Parole chiave**: corrosione, ambiente marino, alta profondità.

Scopo di questa ricerca è quello di indagare gli effetti della corrosione su leghe di Al, Fe, Cu in ambiente marino ad alta profondità. Le leghe analizzate verranno impiegate nel progetto KM3NeT, il cui scopo è quello di costruire una infrastruttura, situata sul fondale marino, in grado di ospitare un telescopio per neutrini.
Per questo studio sono state utilizzate sia leghe di uso comune che materiali di minor uso commerciale.
I campioni sono stati immersi nel sito NEMO (che si trova al largo di Capo Passero, a 3365 m di profondità) per periodi consecutivi di 6, 12 e 18 mesi. Una serie di quattro provini per ciascun tempo di esposizione è stata recuperata e analizzata per valutare il tipo e il grado di corrosione. Gli acciai inossidabili evidenziano le migliori prestazioni in termini di minor perdita di peso, minor velocità di corrosione e attacco localizzato quasi assente. Tuttavia, anche le leghe Al 5093 e Al 6082 hanno prestazioni soddisfacenti, in termini di perdita di peso e velocità di corrosione pur essendo presenti punti di attacco localizzato. Questa preselezione sarà utilizzata nella scelta dei materiali da costruzione per la struttura KM3NeT anche tenendo conto delle prestazioni meccaniche dei materiali esaminati e del loro costo.